Journal of the Korean Magnetic Resonance Society **2019**, *23*, 40-45
DOI 10.6564/JKMRS.2015.23.2.040

Thermodynamic and Physical Properties of $(NH_4)_2MnCl_4{\cdot}2H_2O$ by Nuclear Magnetic Resonance Relaxation Times

Yoo Young Kim *

Department of Science Education, Jeonju University, Jeonju 55069, South Korea

Received May 23, 2019; Revised May 31, 2019; Accepted May 31, 2019

Abstract The phase transition temperatures and thermodynamic properties of $(NH_4)_2MnCl_4{\cdot}2H_2O$ grown by the slow evaporation method were studied using differential scanning calorimetry and thermogravimetric analysis. A structural phase transition occurred at temperature T_{C1} (=264 K), whereas the changes at T_{C2} (=460 K) and T_{C3} (=475 K) seemed to be chemical changes caused by thermal decomposition. In addition, the chemical shift and the spin-lattice relaxation time $T_{1\rho}$ were investigated using ^1H magic-angle spinning nuclear magnetic resonance (MAS NMR), in order to understand the role of NH_4^+ and H_2O. The rise in $T_{1\rho}$ with temperature was related to variations in the symmetry of the surrounding H_2O and NH_4^+.

Keywords $(NH_4)_2MnCl_4{\cdot}2H_2O$, crystal growth, thermodynamic property, phase transition, nuclear magnetic resonance

Introduction

Dihydrate tetrahalogen-metallates ($A_2BX_4{\cdot}2H_2O$) contain the following ions: A (=NH_4, K, Rb, or Cs) and B (=Cu, Mn, Ca, or Ni), which are monovalent and divalent metal ions, respectively, and X (=Cl or Br), which is a halide ion. They crystallize as perovskite-type two-dimensional layered structures.[1-5] The tetrahedrons surrounding the B metal ions at the corners of the unit cell are rotated exactly 90° with respect to the tetrahedron surrounding the ion at the center of the unit cell. The A ions are located in the almost cubic cavities formed by the tetrahedrons.[6,7] $(NH_4)_2MnCl_4{\cdot}2H_2O$, an $A_2BX_4{\cdot}2H_2O$-type compound, undergoes a transition from the high-temperature tetragonal phase to the low-temperature orthorhombic phase at a temperature T_C=270 K.[8] $(NH_4)_2MnCl_4{\cdot}2H_2O$ has a tetragonal structure with space group I4/mmm at room temperature, as shown in Fig. 1.[8] Its unit cell contains two formula units, with lattice constants a=b=7.5250 Å and c=8.276 Å.[9] The water molecules are located on 4-fold axes; hence, the hydrogen positions are crystallographically disordered. The ammonium cations are oriented such that each hydrogen forms weak hydrogen bonds that bridge two edge chlorides of the neighboring octahedral.

Building on previous results, the phase transition and elastic constants of $(NH_4)_2MnCl_4{\cdot}2H_2O$ were investigated by Haussuhl *et al*.[8] Furthermore, the synthesis and structure/property correlations of $(NH_4)_2MnCl_4{\cdot}2H_2O$ in a one-dimensional antiferromagnet were reported by Martin *et al*.[9]

Recently, the structural changes, thermodynamic properties, ^1H magic-angle spinning nuclear magnetic resonance (MAS NMR), and ^{14}N NMR of $(NH_4)_2CuCl_4{\cdot}2H_2O$, which has a structure similar to

* Address correspondence to: **Yoo Young Kim**, Dept. of Science Education, Jeonju University, 303 Chenjam-ro, Wansan-gu, Jeonju-si, 55069, South Korea, Tel: 82-63-220-2554; Fax: 82-63-220-2053; E-mail: yooykim@jj.ac.kr

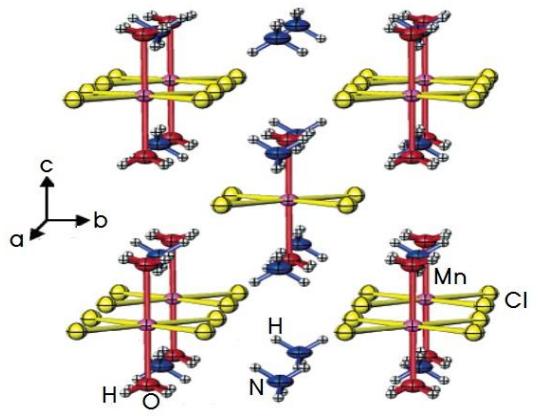

Figure 1. Tetragonal structure of $(NH_4)_2MnCl_4{\cdot}2H_2O$ crystals.

that of $(NH_4)_2MnCl_4{\cdot}2H_2O$, were reported by our groups.[10]

In this study, $(NH_4)_2MnCl_4{\cdot}2H_2O$ crystals were grown using the slow evaporation method, and their crystal structure was determined using X-ray diffraction (XRD). The purpose of this study was to investigate the thermodynamic properties of $(NH_4)_2MnCl_4{\cdot}2H_2O$ single crystals using differential scanning calorimetry (DSC) and thermogravimetric analysis (TGA). Furthermore, the chemical shift and the spin-lattice relaxation time $T_{1\rho}$ in the rotating frame of $(NH_4)_2MnCl_4{\cdot}2H_2O$ were measured using ^1H MAS NMR near the phase transition temperature T_C, focusing on the role of ammonium and water protons. This is the first report on the thermodynamic properties and NMR characteristics of $(NH_4)_2MnCl_4{\cdot}2H_2O$. We have also compared the thermodynamic and physical properties of $(NH_4)_2MnCl_4{\cdot}2H_2O$ determined in this study with those previously reported for $(NH4)_2CuCl_4{\cdot}2H_2O$.

Experimental Methods

$(NH_4)_2MnCl_4{\cdot}2H_2O$ single crystals were grown by slowly evaporating aqueous solutions containing a stoichiometric mixture of NH_4Cl and $MnCl_2{\cdot}2H_2O$ at 300 K. The single crystals were faint pink in color, and hexagonally shaped. The structure of the $(NH_4)_2MnCl_4{\cdot}2H_2O$ crystals at room temperature was determined using XRD (PANalyical X'pert Pro MPD), with a Cu-Kα radiation source, at the Korea Basic Science Institute, Western Seoul Center. The T_C was measured using a Dupont 2010 DSC instrument, at a heating rate of 10°C/min in the temperature range of 170-570 K. The mass of the powdered sample used in the DSC experiment was 7.1 mg. The thermal stability was checked by means of TGA and optical polarizing microscopy. The TGA curve at a heating rate of 10°C/min was measured under N_2 atmosphere, and the mass of the sample used in the TGA experiment was 6.45 mg.

The chemical shifts and the $T_{1\rho}$ in a rotating frame were determined using the ^1H MAS NMR spectra of $(NH_4)_2MnCl_4{\cdot}2H_2O$ measured with a Bruker DSX 400 FT NMR spectrometer at the same facility. The static magnetic field was 9.4 T, and the central radio frequency was set at $\omega_0/2\pi$=400.13 MHz. The powder sample obtained upon grinding the crystals was placed in a 4 mm MAS probe, and the MAS rate was set to 10 kHz, in order to minimize spinning sideband overlap with the central peak. The $T_{1\rho}$ values in the rotating frame were measured using a saturation recovery pulse sequence, sat–t–π/2; the nuclear magnetizations of the ^1H nuclei at time t after the sat pulse, which represent a combination of one hundred π/2 pulses applied at regular intervals, were determined following the π/2 excitation pulse. The width of the π/2 pulse was 3.5 μs for ^1H. The NMR measurements were conducted in the temperature range of 180-430 K. Unfortunately, the chemical shifts and relaxation times could not be measured above 430 K because the NMR spectrometer did not have adequate temperature control at high temperature.

Results and Discussion

The structure of $(NH_4)_2MnCl_4{\cdot}2H_2O$ crystals at room temperature exhibits tetragonal symmetry; this result is consistent with those of previous studies.[9] The DSC curve of the $(NH_4)_2MnCl_4{\cdot}2H_2O$ crystals indicates

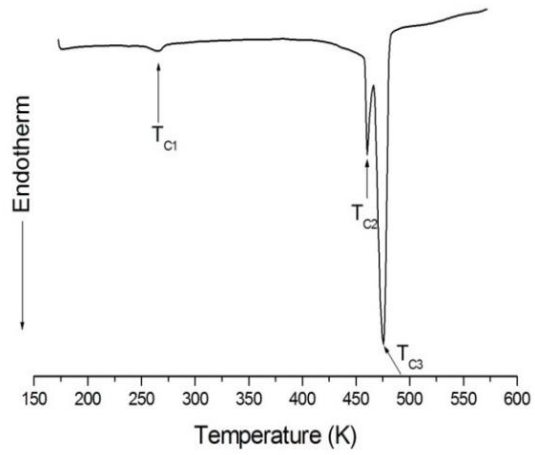

Figure 2. Differential scanning calorimetry (DSC) thermogram of $(NH_4)_2MnCl_4{\cdot}2H_2O$ upon heating

three endothermic peaks during heating, as shown in Fig. 2. The very small peak relative to the other endothermic peaks is present near 264 K (=T_{C1}), and is related to a phase transition. The two endothermic peaks near 460 K (=T_{C2}) and 475 K (=T_{C3}) are related to thermal dehydration due to the loss of H_2O, as suggested below.

TGA analysis was used to understand whether the two endothermic peaks at the high temperatures were structural phase transitions or melting temperatures. The TGA curve of $(NH_4)_2MnCl_4{\cdot}2H_2O$ is shown in Fig. 3. The first occurrence of mass loss begins at approximately 380 K, and 96.81 % of the mass remains at 426 K, yielding $(NH_4)_2MnCl_4{\cdot}1.5H_2O$.

$(NH_4)_2MnCl_4{\cdot}2H_2O$ undergoes a mass loss of 9.57 % at 464 K, and transforms into $(NH_4)_2MnCl_4{\cdot}0.5H_2O$. The bulk mass of $(NH_4)_2MnCl_4{\cdot}2H_2O$ decreases at 380 K (=T_d), which is attributable to the onset of partial thermal decomposition, and undergoes complete thermal decomposition, thereby turning into (NH4)2MnCl4, at approximately 476 K. The endothermic peaks at 460 (=T_{C2}) and 475 K (=T_{C3}) in the DSC experiment are related to the phase transitions from $(NH_4)_2MnCl_4{\cdot}2H_2O$ to $(NH_4)_2MnCl_4{\cdot}0.5H_2O$ and from $(NH_4)_2MnCl_4{\cdot}2H_2O$ to $(NH_4)_2MnCl_4$, respectively. Optical polarizing microscopy indicates that the crystals are transparent at 300 K and vary from

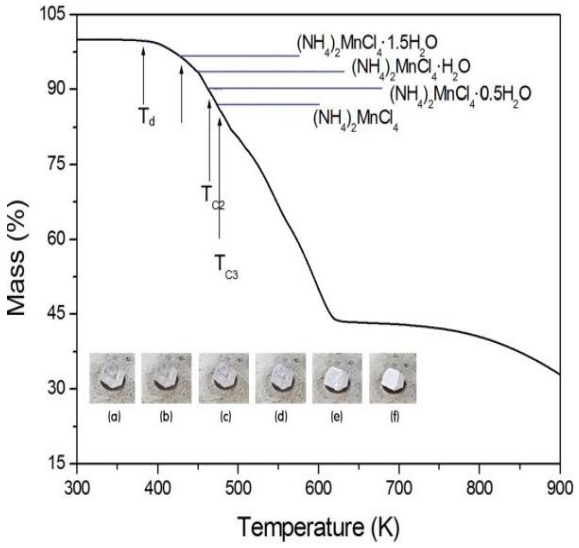

Figure 2. Thermogravimetric analysis (TGA) of $(NH_4)_2MnCl_4{\cdot}2H_2O$ (inset: changes in transparency

transparent (300, 350, and 400 K) to light opaque (420 and 450 K) and opaque (488 K) with an increase in the temperature (inset of Fig. 3). This change may be related to the partial loss of H2O. The weight losses indicated by the TGA curve, near 460 and 475 K, are not related to physical changes such as structural phase transitions.

According to the TGA and optical polarizing microscopy results, the DSC peaks at 460 and 475 K are related to chemical changes due to thermal dehydration.

The ^1H MAS NMR spectra of $(NH_4)_2MnCl_4{\cdot}2H_2O$ were obtained as a function of temperature; the spectrum at 300 K is only one peak at a chemical shift δ=6.66 ppm, as shown in the inset of Fig. 4. The spinning sidebands of the peak are marked with asterisks. There are ammonium and water protons of two kinds in $(NH_4)_2MnCl_4{\cdot}2H_2O$. The NMR experiment could not distinguish the two types of protons because of the overlap of eight protons from ammonium and four protons from water. Therefore, the ^1H NMR signal overlapped by that of the ammonium protons may have included the signal from the water protons. The chemical shifts of the ^1H nuclei in $(NH_4)_2MnCl_4{\cdot}2H_2O$ with respect to tetramethylsilane (TMS) at a frequency of 400.13

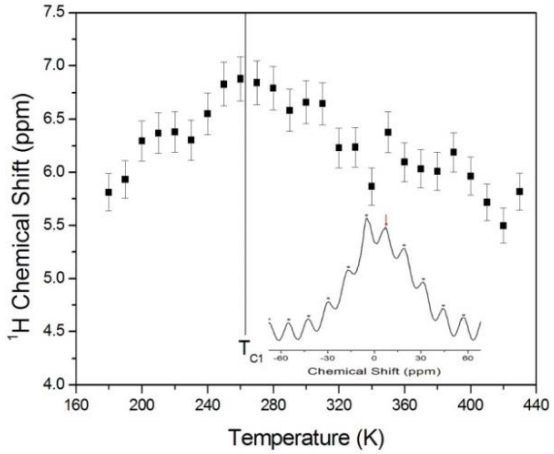

Figure 3. Chemical shift in ^{1}H magic-angle spinning nuclear magnetic resonance (MAS NMR) spectrum of $(NH_4)_2MnCl_4{\cdot}2H_2O$ as a function of temperature (inset: ^{1}H MAS NMR spectrum at 300 K, and spinning sideband is marked with asterisks).

MHz are presented, according to the temperature, in Fig. 4. The chemical shifts of the ^{1}H nuclei increase near T_{C1}, but decrease above T_{C1}. The change in the chemical shift with temperature indicates that the configuration of the atoms neighboring the 1H nuclei undergoes change.

The nuclear magnetization recovery traces for a ^{1}H MAS NMR spectrum are usually represented by a single-exponential function. However, the magnetization recovery traces for the ^{1}H MAS NMR spectrum of $(NH_4)_2MnCl_4{\cdot}2H_2O$ are described using the following double-exponential function.[11-14]

$$P(t)/P0 = 0.5\exp(-t/T_{1\rho}\,(\text{short})) + 0.5\exp(-t/T_{1\rho}\,(\text{long})), \quad (1)$$

where $P(t)$ is the magnetization at time t, and P_0 is the total nuclear magnetization of ^{1}H at thermal equilibrium. Furthermore, $T_{1\rho}$ (short) and $T_{1\rho}$ (long) are the short and long spin-lattice relaxation times, respectively. The magnetization recovery traces according to the delay time ranging from 1 μs to 0.7 ms at temperatures of 190, 270, 350, and 430 K are shown in Fig. 5. The spin-lattice relaxation curves were well fitted by the double-exponential function in Eq. (1), with the slope of the recovery trace decreasing

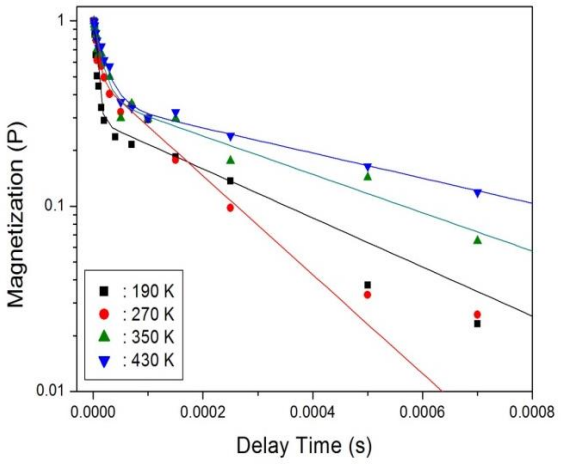

Figure 4. Saturation recovery traces for delay time of ^{1}H in $(NH_4)_2MnCl_4{\cdot}2H_2O$ at 190, 270, 350, and 430 K.

with an increase in the temperature. It is notable that the occurrence of a double-exponential pattern is unusual for a strongly dipolar-coupled proton system, whereas a single-exponential pattern is expected for spin diffusion.[15]

The values of $T_{1\rho}$ for ^{1}H in $(NH_4)_2MnCl_4{\cdot}2H_2O$ at several temperatures are shown in Fig. 6. Two different sets of $T_{1\rho}$ values are obtained using the double-exponential function; the longer values, $T_{1\rho}$ (long), correspond to the ^{1}H in the NH_4^+ groups, whereas the shorter ones, $T_{1\rho}$ (short), correspond to the ^{1}H in the H_2O groups. $T_{1\rho}$ (short) and $T_{1\rho}$ (long) for ^{1}H

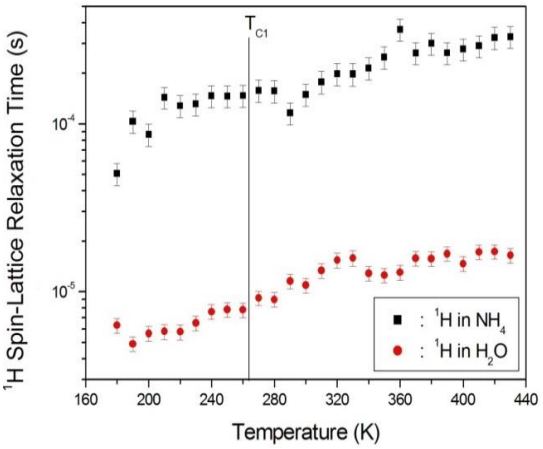

Figure 6. Temperature dependences of the ^{1}H spin-lattice relaxation time in the rotating frame $T_{1\rho}$ for H_2O and NH_4^+ in $(NH_4)_2MnCl_4{\cdot}2H_2O$

Table 1. Phase transition temperatures (T_C), crystal structures, and ^1H spin-lattice relaxation time in the rotating frame ($T_{1\rho}$) values of $(NH_4)_2MnCl_4{\cdot}2H_2O$ and $(NH_4)_2CuCl_4{\cdot}2H_2O$.

	T_C (K)	Crystal structure (at 300 K)	^1H $T_{1\rho}$ (s) (at 300 K)
$(NH_4)_2MnCl_4{\cdot}2H_2O$	264, 460, and 475	Tetragonal	NH_4: 1.5×10^{-4}
			H_2O: 1.1×10^{-5}
$(NH_4)_2CuCl_4{\cdot}2H_2O$	200, 383, and 413	Tetragonal	NH_4: 5.4×10^{-4}
			H_2O: 1.9×10^{-4}

in these groups are continuous near T_{C1}. The rise in $T_{1\rho}$ with temperature contributes to an increase in the mobility of the protons in H_2O and NH_4^+. The changes in the $T_{1\rho}$ values for the ^1H nuclei are related to variations in the environments of H. The structures of the tetrahedrons of water molecules are probably disrupted by the loss of H_2O, as suggested by the TGA experimental results. This indicates that the configuration of ^1H in NH_4^+ and H_2O is temperature-dependent.

We compared the physical properties previously reported for $(NH_4)_2CuCl_4{\cdot}2H_2O$[10] with those determined for $(NH_4)_2MnCl_4{\cdot}2H_2O$ in this study. The difference between these compounds is only the metal ions. $(NH_4)_2MnCl_4{\cdot}2H_2O$ and $(NH_4)_2CuCl_4{\cdot}2H_2O$ are each characterized by three phase transitions (264, 460, and 475 K, and 200, 383, and 413 K, respectively). In addition, the $T_{1\rho}$ values for $(NH_4)_2MnCl_4{\cdot}2H_2O$ are different from those for $(NH_4)_2CuCl_4{\cdot}2H_2O$. The structures and $T_{1\rho}$ values for the two compounds are summarized in Table 1. The ^1H $T_{1\rho}$ values of $(NH_4)_2MnCl_4{\cdot}2H_2O$ are lower than those of $(NH_4)_2CuCl_4{\cdot}2H_2O$. These results indicate that the ^1H $T_{1\rho}$ values of H_2O surrounding Mn^{2+} in $(NH_4)_2MnCl_4{\cdot}2H_2O$ are lower than those of H_2O surrounding Cu^{2+} in $(NH_4)_2CuCl_4{\cdot}2H_2O$. This implies that a short relaxation time is conducive to energy transfer. These differences are due to the differences in the electronic structures of the Mn^{2+} and Cu^{2+} ions, i.e., their d electrons, which screen the nuclear charges from the motion of the outer electrons.[16] Mn^{2+} has unpaired d electrons, whereas Cu^{2+} has one s electron outside the closed d shell. This suggests that the differences between the metal ions are related to the variations in the characteristics of the phase transitions and physical properties.

Conclusions

The phase transitions and thermodynamic properties of $(NH_4)_2MnCl_4{\cdot}2H_2O$ grown by the slow evaporation method were studied using DSC and TGA. The DSC and TGA results indicated that the endothermic peak near 265 K ($=T_{C1}$) was a structural phase transition, whereas the endothermic peaks near 460 K ($=T_{C2}$) and 475 K ($=T_{C3}$) were related to chemical changes following thermal dehydration due to the escape of H_2O; the tetrahedrons formed by the water molecules were probably disrupted by the loss of H_2O. Furthermore, the temperature dependences of the chemical shift and the $T_{1\rho}$ near T_{C1} were obtained; their continuous changes were related to variations in the environments of NH_4^+ and H_2O. The DSC, TGA, and NMR data clearly indicated that the structural change at high temperature was due to the partial loss of the two water molecules coordinated to the Mn^{2+} ion along the c-axis. The ^1H $T_{1\rho}$ values of $(NH_4)_2MnCl_4{\cdot}2H_2O$ were found to be lower than those of $(NH_4)_2CuCl_4{\cdot}2H_2O$ due to the difference in the electronic structures of Mn^{2+} and Cu^{2+} ions.

References

1. N. Narsimlu and K. S. Kumar, *Cryst. Res. Technol*. **37**, 945 (2002)
2. V. D. Franke, Yu. O. Punin, and L. A. P'yankova, *Crystallogr. Rep*. **52**, 349 (2007)
3. Z. Tylczynski and M. Wiesner, *Mater. Chem. Phys.* **149-150**, 566 (2015)
4. Z. Tylczynski, M. Wiesner, and A. Trzaskowska, *Physica* B **500**, 85 (2016)
5. A. R. Lim and J. Cho, *J. Mol. Structure* **1146**, 324 (2017)
6. R. Chidambaram, Q. O. Navarro, A. Garcia, K. Linggoatmodjo, L. S. Chien, and I.-H. Suh, *Acta Cryst*. **B26**, 827 (1970)
7. K. Waizumi, H. Masuda, and H. Ohtaki, *Acta Cryst*. **C48**, 1374 (1992)
8. S. Haussuhl, R. Podeswa, and R. Wagner, *Zeit. Fur Kristallogr*. **173**, 139 (1985)
9. J. D. Martin, R. F. Hess, and P. D. Boyle, *Inorg. Chem*. **43**, 3242 (2004)
10. A.R. Lim and S.H. Kim, *RSC Adv.* **8**, 6502 (2018)
11. J. L. Koenig, *Spectroscopy of Polymers*, Elsevier, New York, 1999
12. A. Abragam, *The Principles of Nuclear Magnetism*, Oxford University Press, London, 1961
13. B. Cowan, *Nuclear Magnetic Resonance and Relaxation*, Cambridge University, UK, 1997
14. T.H. Yeom, *J. Korean Mag. Res. Soc*. **22**, 107 (2018)
15. A.R. Lim, S.W. Kim and Y.L. Joo, *J. Appl. Phys*. **121**, 215501 (2017)
16. A.R. Lim, *RSC Adv.*, **8**, 18656 (2018)